International Journal of Engineering

Journal Homepage: www.ije.ir

Wave Energy Dissipation Using Perforated and Non Perforated Piles

M. Feizbahr*[a], C. Kok Keong[a], F. Rostami[b], M. Shahrokhi[c]

[a] *School of Civil Engineering, Engineering Campus, University Sains Malaysia, Nibong Tebal , Penang, Malaysia*
[b] *Department of Civil Engineering, North Tehran branch, Islamic Azad university, Tehran, Iran*
[c] *Ghiaseddin Jamshid Kashani Higher Education Institute, Iran*

P A P E R I N F O

Paper history:
Received 06 July 2017
Received in revised form 27 September 2017
Accepted 12 October 2017

Keywords:
Breakwater
Perforation
Hollow Piles
Flow 3D
Wave Modeling
Coastal-Protection

A B S T R A C T

The indispensable vital structure in any harbor is a breakwater in order to make available calm water region inshore. Pile breakwater can be employed as small coastal-protection structure where tranquility required is low. This study is concerned with CFD study on performance of perforated hollow pile to dissipate wave energy and the novelty of this investigation is the role of perforation layout to dissipate energy of water. Pile models under two different incident waves with constant water depth and wave amplitude have been classified into two groups with two different wavelengths, making a total of 10 models which has been simulated numerically by computational flow solver FLOW 3D. The analytical results of simulations show changes in the velocity profiles after piles while dissipation happened in the vicinity of the pile. The results implied that the perforated models can perform better than the non-perforated ones and energy dissipation was found much more significant in perforated piles because dissipation goes on for about 2.5 m after the pile for the perforated case, while for the non-perforated case this distance reduce to 1.5 m after pile.

***doi**: 10.5829/ije.2018.31.02b.04*

1. INTRODUCTION

Pile breakwaters are frequently employed as small coastal-protection structures. Any fishing harbors, marinas, recreational coasts, dock, etc., where tranquility required is low, piles can be used as simple breakwater [1-3]. The important advantages of these types are: i. relatively low cost in comparison with the other types. ii. occupation of small area and iii. less safeguarding cost; the most conventional solution in deeper waters; successfully employed for low and moderate wave energy applications; not harmful for sea wildlife; water flow circulation between to separated zone by piles and continuous refreshing the harbor area water and pollution prohibition [4, 5]. They have long been employed with different design methods. When full wave protection is not required, pile breakwaters have extensive use in near shore line with a variety of shapes and performance [6]. Various laboratory investigations of hydraulic characteristics of pile breakwaters has been done to extend the real-world engineering requirements [4, 7-9].

Since the early study of Jarlan [10] on the effect of a single perforated wall in front of a breakwater in damping waves, many researchers have investigated the interaction of waves with perforated structures. Perforated material improves damping effect by absorption and dissipation of the wave energy when the incident wave transmits over it [11-14]. Rao et al. [15] have carried out an experimental investigation on perforated hollow piles with two rows pattern in a two dimensional wave flume and results were compared with non-perforated piles under identical conditions i.e. the same water depth, incident wave, clear spacing between the piles and the spacing of pile rows on transmission coefficient. Results show the increase in wave energy dissipation for two rows of non-perforated piles compared to a single row.

Based on the above observation by Rao et al. [15], this study has been carried out to investigate the effect of perforation in pile on dissipation of energy by means of CFD analysis. Only two aspects of layout of suitable chosen perforation with specific size on a single hollow

*Corresponding Author's Email: *m.feizbahr@gmail.com* (M. Feizbahr)

Please cite this article as: M. Feizbahr, C. Kok Keong, F. Rostami, M. Shahrokhi, Wave Energy Dissipation Using Perforated and Non Perforated Piles, International Journal of Engineering (IJE), IJE TRANSACTIONS B: Applications Vol. 31, No. 2, (February 2018) 212-219

pile has been studied in order to yield more basic details on the relative perforation of piles with and without perforation in dissipating energy.

2. GOVERNING EQUATIONS

The problem solved in this study is an initial-boundary-value problem. The problem is solved by means of computational fluid dynamic analysis. In this section, the basic equations used are briefly given.

The basic equations used in CFD are the following Navier-Stokes equations of motion for the fluid velocity components (u, v, w) in the three coordinate directions:

$$\frac{\partial u}{\partial t}+\frac{1}{v_F}\left\{uA_x\frac{\partial u}{\partial x}+vA_y\frac{\partial u}{\partial y}+wA_z\frac{\partial u}{\partial z}\right\}=-\frac{1}{\rho}\frac{\partial p}{\partial_x}+G_x+f_x$$

$$\frac{\partial v}{\partial t}+\frac{1}{v_F}\left\{uA_x\frac{\partial v}{\partial x}+vA_y\frac{\partial v}{\partial y}+wA_z\frac{\partial v}{\partial z}\right\}=-\frac{1}{\rho}\frac{\partial p}{\partial_y}+G_y+f_y \quad (1)$$

$$\frac{\partial w}{\partial t}+\frac{1}{v_F}\left\{uA_x\frac{\partial w}{\partial x}+vA_y\frac{\partial w}{\partial y}+wA_z\frac{\partial w}{\partial z}\right\}=-\frac{1}{\rho}\frac{\partial p}{\partial_z}+G_z+f_z$$

where, A_x is fractional area open to flow in the x-direction. Similar for y and z direction, A_y and A_z are similar area fractions for flow in the y and z directions, respectively. (Gx, Gy, Gz) are body and (fx, fy, fz) viscous accelerations, respectively. For a variable dynamic viscosity μ, the viscous accelerations are:

$$\rho V_f f_x=wsx-\left\{\frac{\partial}{\partial x}\left(A_{xx}\right)+\frac{\partial}{\partial y}\left(A_{xy}\right)\right\}+\frac{\partial}{\partial z}\left(A_{xz}\right)$$

$$\rho V_f f_x=wsy-\left\{\frac{\partial}{\partial x}\left(A_{xy}\right)+\frac{\partial}{\partial y}\left(A_{xy}\right)\right\}+\frac{\partial}{\partial z}\left(A_{xyz}\right) \quad (2)$$

$$\rho V_f f_x=wsz-\left\{\frac{\partial}{\partial x}\left(A_{xxz}\right)+\frac{\partial}{\partial y}\left(A_{xyz}\right)\right\}+\frac{\partial}{\partial z}\left(A_{xzz}\right)$$

where:

$$\tau_{xx}=-2\mu\left\{\frac{\partial u}{\partial x}-\frac{1}{3}\left(\frac{\partial u}{\partial x}+\frac{\partial v}{\partial y}+\frac{y_w}{\partial z}\right)\right\}$$

$$\tau_{xx}=-2\mu\left\{\frac{\partial v}{\partial y}-\frac{1}{3}\left(\frac{\partial u}{\partial x}+\frac{\partial v}{\partial y}+\frac{y_w}{\partial z}\right)\right\} \quad (3)$$

$$\tau_{xx}=-2\mu\left\{\frac{\partial w}{\partial x}-\frac{1}{3}\left(\frac{\partial u}{\partial x}+\frac{\partial v}{\partial y}+\frac{y_w}{\partial z}\right)\right\}$$

$$\tau_{xy}=-\mu\left\{\frac{\partial v}{\partial y}+\frac{\partial u}{\partial x}\right\}$$

$$\tau_{xz}=-\mu\left\{\frac{\partial u}{\partial z}+\frac{\partial w}{\partial x}\right\}$$

$$\tau_{yz}=-\mu\left\{\frac{\partial v}{\partial z}+\frac{\partial w}{\partial y}\right\}$$

In the above expressions, the terms *wsx*, *wsy* and *wsz* are wall shear stresses. If these terms are omitted, there is no wall shear stress because the remaining terms contain the fractional flow areas (*Ax*, *Ay*, *Az*) which vanish at the walls. The wall stresses are modeled by assuming a zero tangential velocity on the portion of any area closed to flow.

In CFD, the Navier-Stokes and continuity equation are discretized and solved for each computational cell which are used to represent the domain where fluid mechanics problem is to be solved [16-18]. In this study, it is the fluid domain of the flow within a flume bounded by the wall of the flume, the starting and ending section of the flume and the solid-fluid boundary defined by the surface between the fluid and the hollow pile model with and without perforation.

3. NUMERICAL MODELING

A periodic linear surface wave can be generated at a mesh boundary. The model is based on Airy's linear wave theory. The linear wave is assumed to come from a flat bottom reservoir into the computational domain. A linear wave is characterized by the wave amplitude A, wavelength λ, angular frequency ω and wave number $k=2\pi/\lambda$ (Figure 1).

The linear wave theory is based on the following assumptions:

i. Fluid is incompressible, in viscid, irrational, two-dimensional flow
ii. The wave amplitude (A) is small compared to the water depth (h) and wavelength (λ)

With the above assumptions, the problem can be reduced to a linear potential flow problem.

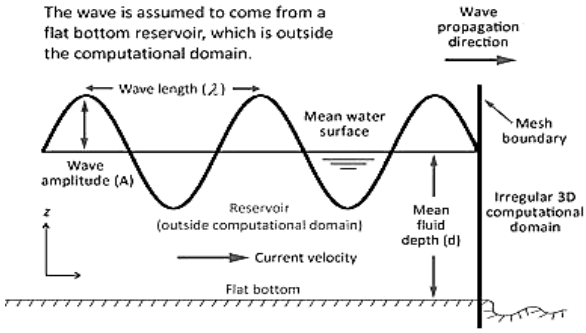

Figure 1. Wave propagation properties (Flow 3D)

The free surface elevation η(x, t) measured in the vertical direction from mean water surface, the velocity potential f (x, z, t), and velocity components in x and z directions u(x, z, t) and w(x, z, t) are obtained as

$$\eta = A\cos\left(k_x - \omega t + \phi\right) \tag{4}$$

$$\varphi\left(x,z,t\right) = xU + \frac{A\omega\cos h\left[k\left(z+h\right)\right]\sin\left(kx-\omega t+\phi\right)}{k\sin h\left(kh\right)}$$

$$u\left(x,z,t\right) = U + \frac{A\omega\cos h\left[k\left(z+h\right)\right]\cos\left(kx-\omega t+\phi\right)}{\sin h\left(kh\right)} \tag{5}$$

$$\omega\left(x,z,t\right) = \frac{A\omega\sin h\left[k\left(z+h\right)\right]\sin\left(kx-\omega t+\phi\right)}{k\sin h\left(kh\right)}$$

where, φ the phase shift angle, t time, and h the mean depth of the fluid. The dispersion equation in terms of wave speed c = ω/k is given by:

$$\left(c-U\right)^2 = \frac{g}{k}\tan h\left(kh\right) \tag{6}$$

The following relationship indicates that the wave frequency and wave length are not independent, but are related:

$$\omega^2\left(1-\frac{kU}{\omega}\right)^2 = \frac{2\pi g}{\lambda}\tanh\frac{2\pi g}{\lambda} \tag{7}$$

It is generally accepted that dissipation processes are the least well-represented in numerical wave models [19]. Turbulent kinetic Energy (TKE) is generated from fluctuation in velocity of the ocean system and a fraction of TKE is dissipated and remainder is used to increase the potential energy. The one-equation turbulence transport model consists of an equation for the kinetic energy associated with turbulent velocity fluctuations in the flow (the turbulent kinetic energy).

The one-equation turbulence transport model consists of a transport equation for the specific kinetic energy associated with turbulent velocity fluctuations in the flow (the turbulent kinetic energy):

$$K_T = \tfrac{1}{2}((\acute{u}^2)^- + \overline{\acute{v}^2} + \overline{\acute{w}^2}) \tag{8}$$

where, *u'*, *v'*, *w'* are the x-, y-, z-components of the fluid velocity associated with messy turbulent fluctuations. As can be seen from the above mentioned equation of kinetic energy, the energy in a flow is clearly related to the velocity of the flow. Therefore, the change in velocity of flow before and after hollow pile has been checked to examine the relative performance in term of energy dissipation. Direct calculation of energy is not carried out as mentioned earlier. The model is used in this study is a flume of height H=0.9m and length L=15m and width B=0.2m with a stationary hollow pile located at the distance of *l*= 6m from the start of the flume.

As mentioned earlier, perforated circular hollow sections has been modeled together with a B×H×L flume with height 0.90 m, outer diameter 0.150 m and wall thickness l0mm (Figure 2). The pile model is placed exactly at the middle of mesh block 2, with the x, y, and z coordinate of respectively 6.00, 0.1, and 0.00. Since the pile is considered stationary in the flow within the flume, it has been considered in the CFD analysis as solid – fluid boundary. Perforation with circular shape is chosen. The diameter is 0.05 m corresponding to a constant ratio of 1/3 with outer diameter of pile.

Two positions have been considered for perforation location: the centers of their perforation are difference in terms of the location at 0.4 m and 0.327 m from bed of flume. In total, five cases of analysis with different hollow pile in terms of their perforation layout have been generated (Figure 2). All five cases have been analyzed under two different wave period denoted as P0.75 and P1.5, respectively (Table 1).

In order to simulate the flume, four blocks have been generated as mentioned earlier. These four blocks are meshed with different cell sizes and boundary conditions. Mesh block 1, 2, 3 and 4 are all cubical in shape. In order to have more accurate results, mesh block 2 wherein the pile model is located, has been assigned with the highest mesh density which has been detailed in Figure 3.

Initial wave is generated with wave boundary condition in mesh block 1. Wave attribute is explained in (Table 1).

Initial conditions used in the analysis conforms to those used in the experimental study of [15] on perforated hollow piles.

Highly turbulent wave has been modeled as a Newtonian viscosity and turbulent. k-ε Equation is used to generate vortex currents, three-dimensional boundary layers, water jets, etc. [20].

$$\frac{\partial}{\partial t}(\rho k) + \frac{\partial}{\partial x_{ih}}(\rho k u_i) = \frac{\partial}{\partial x_j}\left[\left(\mu + \frac{\mu_t}{\sigma_k}\right)\frac{\partial k}{\partial x_j}\right] + G_k - \rho\varepsilon \tag{9}$$

$$\frac{\partial}{\partial t}(\rho\varepsilon) + \frac{\partial}{\partial x_i}(\rho\varepsilon u_i) = \frac{\partial}{\partial x_j}\left[\left(\mu + \frac{\mu_t}{\sigma_\varepsilon}\right)\frac{\partial \varepsilon}{\partial x_j}\right] + C_{1\varepsilon}\frac{\varepsilon}{k}G_k - c_{2\varepsilon}\rho\frac{\varepsilon^2}{k} \tag{10}$$

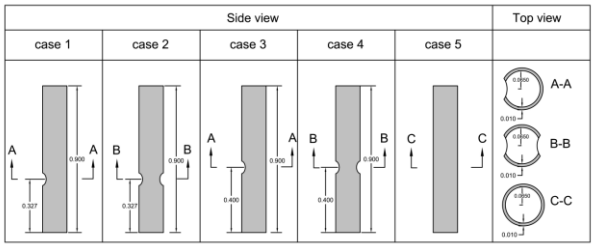

Figure 2. Different perforated hollow species

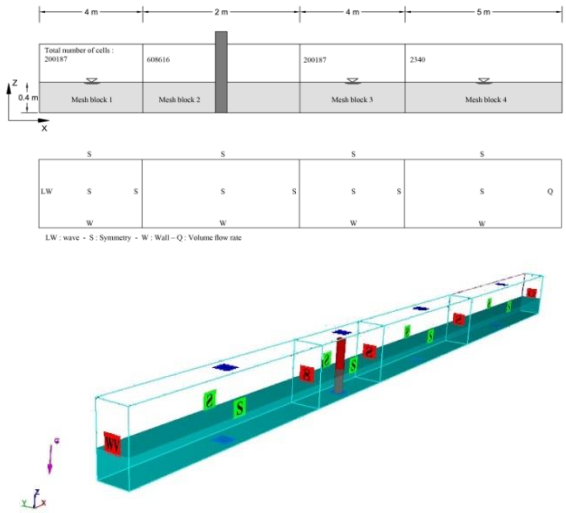

Figure 3. Mesh blocks 1, 2, 3 and 4

TABLE 1. Wave definition

Wave attributes			
Mean fluid depth(m)	Wave amplitude(m)	Wave period(sec)	Phase shift
0.4	0.1	0.75, 1.5	0

where $C_{\mu} = 0.09$, $C_{1\varepsilon} = 1.44$, $C_{2\varepsilon} = 1.92$, $\sigma_k = 1.0$, $\sigma_{\varepsilon} = 1.3$ are the constant values.

For the purpose of studying dissipation energy of wave by the use of perforated hollow piles, velocity of flow has been used as a measure to represent kinetic energy of flow. In this study, results of X velocity are examined to discuss about the energy of progressive wave, where X corresponds to longitudinal direction of the flume. For this study, 10 models have been analyzed. The models have been categorized by the wave period and pile cases, Tables 2 and 3.

3. 1. Verification Test

Wave generated experimentally by Vincent and Briggs [21], has been considered to verify the wave simulated by the software. The test was carried out in a wave generator with the surface area of 35m × 29m, while the water depth over

TABLE 2. Analysis model categories for wave period of 0.75 s (Group 1)

	hole numbers	Depth from flume bed
case 1	1	0.4
case 2	2	0.4
case 3	1	0.327
case 4	2	0.327
case 5	Non-perforated	

TABLE 3. Analysis model categories for wave period of 1.5 s (Group 2)

	hole numbers	Depth from flume bed
case 1	1	0.4
case 2	2	0.4
case 3	1	0.327
case 4	2	0.327
case 5	Non-perforated	

the shoal is:

$$-0.4572+0.7620\left[1-\left(\frac{x'}{3.81}\right)^2-\left(\frac{z'}{4.95}\right)^{0.5}\right] \quad (11)$$

(where in the above equation, X' and Y' are the localized coordinates on the elliptical shoal which representing minor and major axes respectively.)

For the other areas is 45.72cm. The elliptical shoal was defined with major radius of 3.96m and minor radius of 3.05m and the height of 30.48cm at the center.

Wave height ratio H/Hi has been computed with k-ε and RNG turbulence models with the information given in Table 4. Figure 4 shows a comparison between the results of the numerical models and laboratory data by Vincent and Briggs [21].

The numerical results present almost good agreement with experimental data, although some differences is clear between the trends, the result of k-ε model shows acceptable accuracy.

TABLE 2. Wave definition

Case ID	Period (sec)	Height (cm)
a	1.33	5.5
b	1.33	2.54
c	1.33	13.5

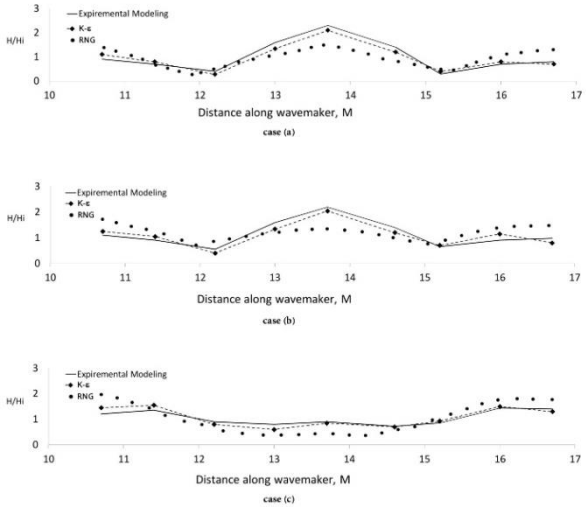

Figure 4. Comparison of experimental data with CFD k-ε and RNG turbulence models

4. RESULTS AND DISCUSSION

Wave kinetic energy dissipation due to perforated and non-perforated piles has been investigated numerically with a computational flow solver (FLOW 3D). Velocity profile (Figures 5 and 6) illustrated with non-dimensional parameters of depth and velocity $U_{Average}$ and U_{max} calculated for each section.

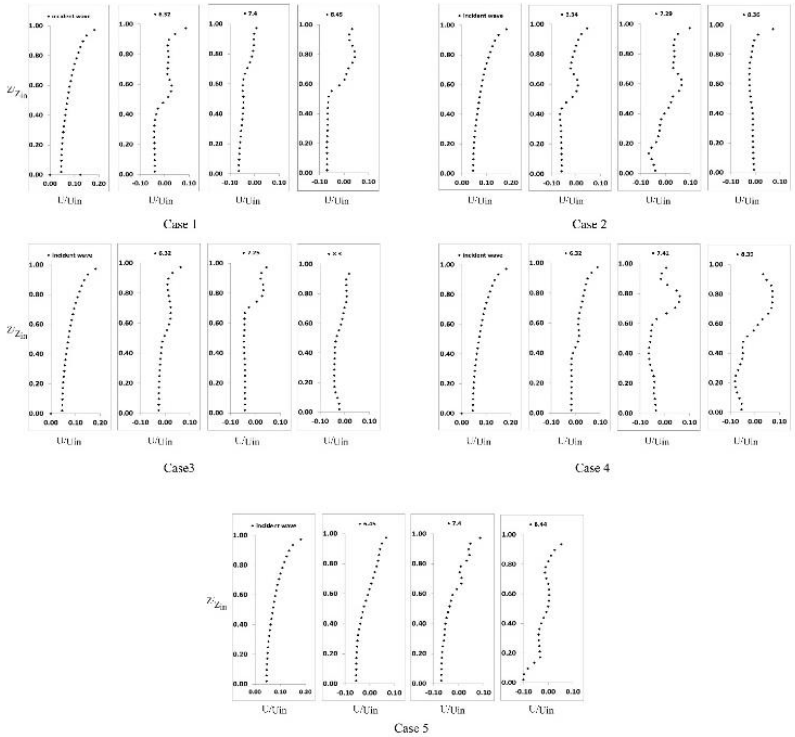

Figure 5. Vertical distribution of velocity profiles for wave period of 0.75 *s*

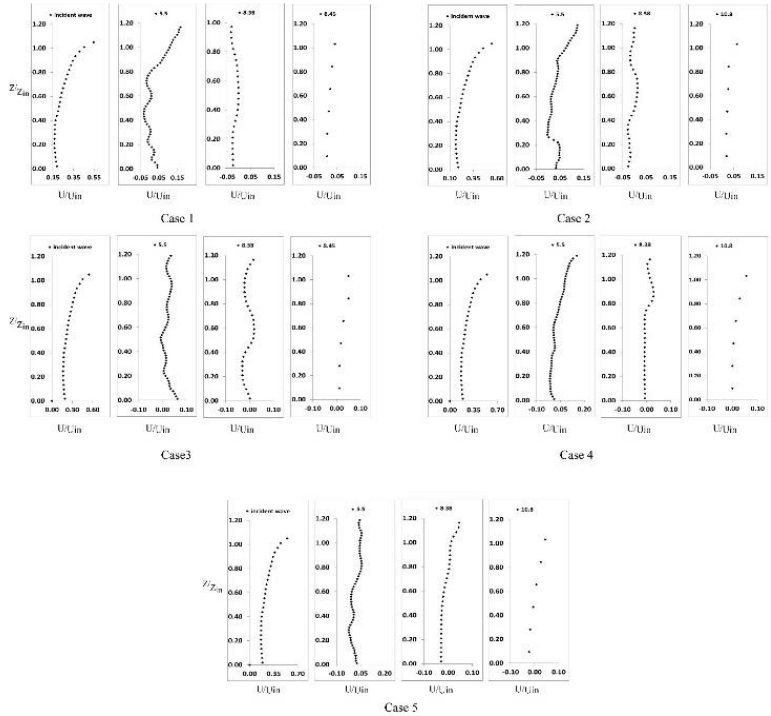

Figure 6. Vertical distribution of velocity profiles for wave period of 1.5 sec

Moreover, the reduction rates of velocity in some sections after the pile are calculated. Comparison of the values of $U_{Average}$ show that in all cases velocity decreased almost between 68 to 120% in deferent sections for wave period of 0.75 s and 79 to 102% for wave period of 1.5s. The $U_{Average}$ is obtained by the following formula:

$$U_{average} = \frac{\sum u_i \left(z_i - z_{i-1}\right)}{H} \quad (12)$$

where, H is flow depth, u_i is x-direction velocity component in the i^{th} point in flow with height of z_i. In wave period of 0.75 s, the highest dissipation happened for the case 1 while for wave period of 1.5s the highest happened for case 3 model. In the most cases, the lowest reduction occurs at the third wave in comparison with the other two wave periods.

Velocity profile for wave period of 0.75 sec and U_{max} and corresponding depths are presented in Tables 5 and 6. These values indicate that in most cases trend value suddenly increases beneath the pile perforation and this phenomenon is higher in the two sides perforated pile because of jetting water through the hole while wave get far from the pile this phenomenon come up to the water surface. Eddies induced by the water jet, may cause turbulences, which results in negative velocity and energy dissipation.

With the exception of the Case 1, in both wave periods, the non-perforated performance was obviously better than perforated piles in the terms of $U_{Average}$. In the case of wave period of 1.5 *s*, at the two first incident waves, in the near surface region, flow velocity decrease gradually or remain constant in comparison with near bed velocity.

The contours of kinetic energy for the group 1 presented in Figures 7 and 8. These figures show that highest values of energy dissipation happen at Cases 1 and 3, and for wave period of P1.5 it happens at Case 2. However, the effect of pile for P0.75 series is higher than P1.5 series, which particularly its energy is close to zero, exactly after the pile and this procedure continue for P0.75 up to 2.5m after pile and then gradually will increase; so, the tendency of lower wave period to dissipate the kinetic energy by this breakwater system is perceptibly higher. As it is clear in Figures 5 and 6, because of its far distance from the pile, tranquility happens after a high turbulence around the pile and reduction of reverse velocity due to the small eddies in those areas produce waves with higher values of $U_{average}$ of P0.75s, and also for P1.5s, while for P1.5s the rate of energy alteration starts in 1.5m after pile.

TABLE 5. Wave speed alteration in during flume for wave period of 0.75 *s*

	Incoming wave			1st wave				2nd wave				3th wave			
	U max	Z	U ave	U max	Z	U ave	Velocity reduction (%)	U max	Z	U ave	Velocity reduction (%)	U max	Z	U ave	Velocity reduction (%)
case 1	0.166	3.43	0.16	0.378	0.23	0.016	89.988	-0.004	0.34	-0.033	120.625	0.057	0.31	-0.022	113.750
case 2	0.166	3.43	0.16	0.010	0.23	0.016	90.125	0.086	0.23	0.022	86.313	-0.001	0.00	0.008	95.313
case 3	0.166	3.43	0.16	0.031	0.26	0.018	88.750	0.043	0.32	0.020	87.500	0.011	0.31	0.024	85.000
case 4	0.166	3.43	0.16	0.089	0.37	0.051	68.125	0.081	0.31	0.014	91.000	0.095	0.32	0.027	83.000
case 5	0.166	3.43	0.16	0.055	0.35	0.003	97.875	0.057	0.34	0.000	99.983	0.034	0.35	0.007	95.438

TABLE 6. Wave speed alteration in during flume for wave period of 1.5 *s*

	Incoming wave			1st wave				2nd wave				3th wave			
	U max	Z	u ave	U max	Z	u ave	velocity reduction (%)	U max	Z	u ave	velocity reduction (%)	U max	Z	u ave	velocity reduction (%)
case 1	0.012	0.400	0.497	0.250	0.440	0.084	83.099	0.066	0.460	-0.012	102.394	0.070	0.410	0.072	85.513
case 2	0.119	0.400	0.497	0.023	0.480	0.100	79.879	0.024	0.260	0.020	95.976	0.040	0.330	0.105	78.873
case 3	0.119	0.400	0.497	0.110	0.000	0.047	90.543	0.033	0.230	0.003	99.497	0.086	0.340	0.080	83.903
case 4	0.119	0.400	0.497	0.202	0.450	0.100	79.879	0.049	0.350	0.016	96.781	0.096	0.410	0.052	89.537
case 5	0.119	0.400	0.497	0.096	0.330	0.060	87.928	0.079	0.460	0.013	97.384	0.075	0.410	0.039	92.153

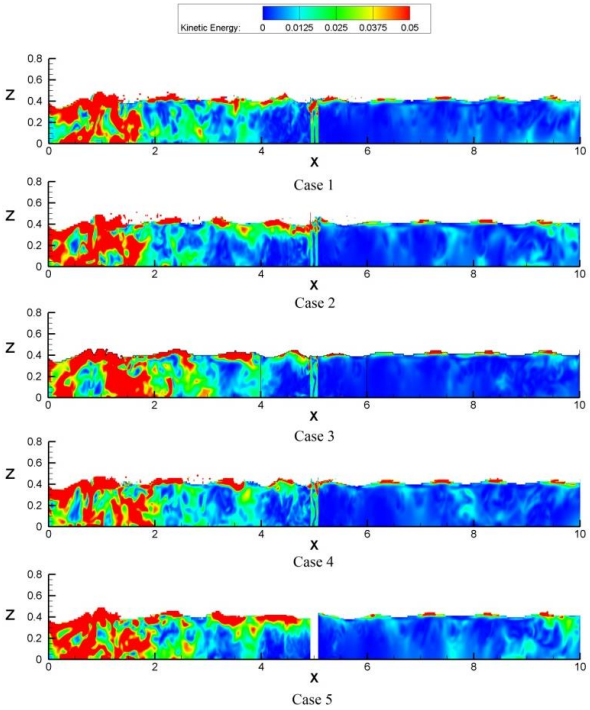

Figure 7. Kinetic energy counters (group 1)

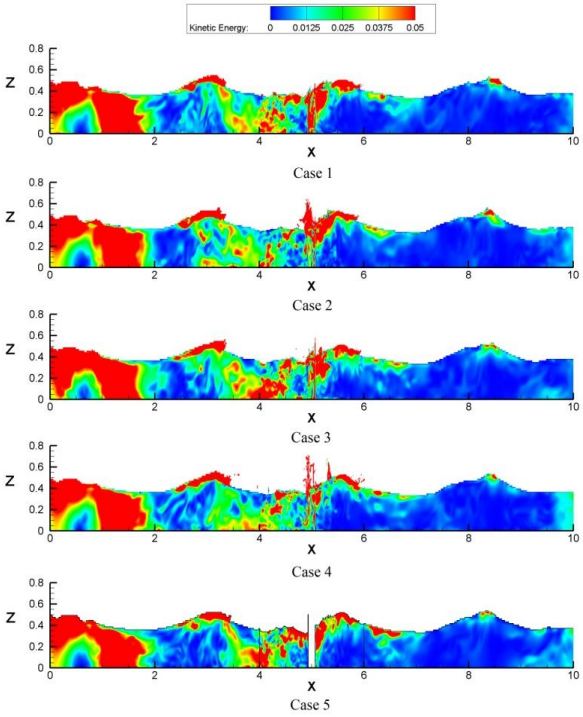

Figure 8. Kinetic energy counters (group 2)

The kinetic energy counters also show that in Cases 1 and 3, rising in wave energy happen in farther distance in comparison with Cases 2 and 4 in wave period. Figures 5 and 6 also shows the area with higher kinetic energy by getting far from the piles both in wave period of 0.75 and 1.5 s.

5. CONCLUSION

This study has been carried out to investigate the capability of the perforation to dissipate energy of wave. It has also been carried out to determine the effect of layout of perforation in hollow pile to dissipate energy of wave. A total of 10 models of circular hollow piles were analyzed. They consisted of two controlled models without perforation and 8 models with perforation with different layout. Analyses have been carried out by two different wave periods of 0.75 and 1.5 to satisfy the objective of this study. The results of this analysis indicate that performance of perforated piles of Cases 1 and 3 in both wave periods, *P 0.75s* and *P 1.5 s*, satisfy the objective. It is also clear that pile break water can be always a candidate to dissipate kinetic energy for the shorter wave length. The results also showed that both for perforated and non-perforated cases, energy dissipation occurred exactly after pile for *P 0.75 s* and this dissipation goes on for about 2.5 *m* after the pile for perforated case, while for *non-perforated case this* distance reduce to 1.5 m after pile.

6. REFERENCES

1. Koraim, A.S.I., "Suggested model for the protection of shores and marina", Zagazig University, Zagazig, Egypt, (2005).
2. Ji, C.-H. and Suh, K.-D., "Wave interactions with multiple-row curtainwall-pile breakwaters", ***Coastal Engineering***, Vol. 57, No. 5, (2010), 500-512.
3. Zhu, D., "Hydrodynamic characteristics of a single-row pile breakwater", ***Coastal Engineering***, Vol. 58, No. 5, (2011), 446-451.
4. Suh, K.-D., Shin, S. and Cox, D.T., "Hydrodynamic characteristics of pile-supported vertical wall breakwaters", ***Journal of waterway, port, coastal, and ocean engineering***, Vol. 132, No. 2, (2006), 83-96.
5. Hutchinson, P. and Raudkivi, A., Case history of a spaced pile breakwater at half moon bay marina auckland, new zealand, in Coastal engineering, (1984). 1985.2530-2535.
6. Jiang, C., Yao, Y., Deng, Y. and Deng, B., "Numerical investigation of solitary wave interaction with a row of vertical slotted piles", ***Journal of Coastal Research***, Vol. 31, No. 6, (2015), 1502-1511.
7. Hayashi, T., Hattori, M., Kano, T. and Shirai, M., "Hydraulic research on the closely spaced pile breakwater", ***Coastal Engineering in Japan***, Vol. 9, No. 1, (1966), 107-117.
8. Kakuno, S. and Liu, P.L.-F., "Scattering of water waves by vertical cylinders", ***Journal of Waterway, port, Coastal, and Ocean Engineering***, Vol. 119, No. 3, (1993), 302-322.
9. Suh, K.-D., Jung, H.Y. and Pyun, C.K., "Wave reflection and transmission by curtainwall–pile breakwaters using circular

piles", ***Ocean Engineering***, Vol. 34, No. 14-15, (2007), 2100-2106.

10. Jarlan, G., "A perforated vertical wall breakwater", ***The Dock and Harbour Authority***, No. 486, (1961), 394-398.
11. Tsai, C.-P., Chen, H.-B. and Lee, F.-C., "Wave transformation over submerged permeable breakwater on porous bottom", ***Ocean Engineering***, Vol. 33, No. 11-12, (2006), 1623-1643.
12. Liu, Y., Li, Y.-c. and Teng, B., "Wave interaction with a perforated wall breakwater with a submerged horizontal porous plate", ***Ocean Engineering***, Vol. 34, No. 17-18, (2007), 2364-2373.
13. Nikoo, M.R., Varjavand, I., Kerachian, R., Pirooz, M.D. and Karimi, A., "Multi-objective optimuma design of double-layer perforated-wall breakwaters: Application of nsga-ii and bargaining models", ***Applied Ocean Research***, Vol. 47, (2014), 47-52.
14. Mirbagheri, S., RAJAEI, T. and MIRZAEI, F., "Solution of wave equations near seawalls by finite element method", ***International Journal of Engineering Transactions A Basics***, Vol. 21, No. 1, (2008), 1-16.
15. Rao, S., Rao, N. and Sathyanarayana, V., "Laboratory investigation on wave transmission through two rows of perforated hollow piles", ***Ocean Engineering***, Vol. 26, No. 7, (1999), 675-699.
16. Rostami, F., Shahrokhi, M., Said, M.A.M. and Abdullah, R., "Numerical modeling on inlet aperture effects on flow pattern in primary settling tanks", ***Applied Mathematical Modelling***, Vol. 35, No. 6, (2011), 3012-3020.
17. Rostami, F., Shahrokhi, M., Saod, M.A.M. and Yazdi, S.R.S., *Retracted: Numerical simulation of undular hydraulic jump on smooth bed using volume of fluid method*. (2013), Elsevier.
18. Bin, Y.O., Tawi, K. and Suprayogi, S.D., "Computer simulation studies on the effect overlap ratio for savonius type vertical axis marine current turbine", (2010).
19. Cavaleri, L., Alves, J.-H., Ardhuin, F., Babanin, A., Banner, M., Belibassakis, K., Benoit, M., Donelan, M., Groeneweg, J. and Herbers, T., "Wave modelling–the state of the art", ***Progress in Oceanography***, Vol. 75, No. 4, (2007), 603-674.
20. Jones, A. and Launder, D., *Lectures in mathematical models of turbulence*. (1972), London: Academic Press.
21. Vincent, C.L. and Briggs, M.J., "Refraction—diffraction of irregular waves over a mound", ***Journal of Waterway, Port, Coastal, and Ocean Engineering***, Vol. 115, No. 2, (1989), 269-284.

Wave Energy Dissipation Using Perforated and Non Perforated Piles

M. Feizbahr[a], C. Kok Keong[a], F. Rostami[b], M. Shahrokhi[c]

[a] *School of Civil Engineering, Engineering Campus, University Sains Malaysia, Nibong Tebal , Penang, Malaysia*
[b] *Department of Civil Engineering, North Tehran branch, Islamic Azad university, Tehran, Iran*
[c] *Ghiaseddin Jamshid Kashani Higher Education Institute, Iran*

P A P E R I N F O

Paper history:
Received 06 July 2017
Received in revised form 27 September 2017
Accepted 12 October 2017

Keywords:
Breakwater
Perforation
Hollow Piles
Flow 3D
Wave Modeling
Coastal-Protection

چکیده

یکی از سازه های حیاتی برای آرام نگاه داشتن ساحل بنادر موج شکن است . موج شکن شمعی می تواند به عنوان سازه‌ی محافظ برای سواحلی که دارای امواج آرام هستند استفاده شود . این تحقیق به بررسی عددی اتلاف انرژی توسط موج شکن های شمعی سوراخ دار و بدون سوراخ به ویژه آرایش هندسی سوراخ ها در اتلاف موج پرداخته است . مدل های شمع تحت با عمق آب و دامنه موج ثابت در دو گروه با دو طول موج مختلف طبقه بندی شده اند. و به طور کلی تعداد ۱۰ مدل توسط نرم افزار FLOW 3D شبیه سازی گردید. نتایج تحلیل های انجام شده نشان می دهد که اتلاف انرژی بعد از شمع ها و در نزدیکی شمع اتفاق افتاده است. نتایج همچنین نشان می دهد که مدل های سوراخ دار اتلاف انرژی بهتری را نسبت به مدل شاهد بدون سوراخ داشتند.

***doi**: 10.5829/ije.2018.31.02b.04*